

# Essential-State Model for Polymethine Dyes: Symmetry Breaking and Optical Spectra

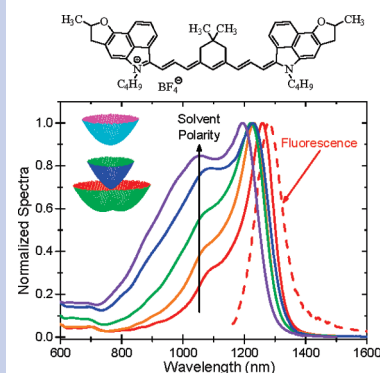
Francesca Terenziani,<sup>†</sup> Olga V. Przhonska,<sup>§,†</sup> Scott Webster,<sup>‡</sup> Lazaro A. Padilha,<sup>‡</sup> Yuriy L. Slominsky,<sup>‡</sup> Iryna G. Davydenko,<sup>‡</sup> Andriy O. Gerasov,<sup>‡</sup> Yuriy P. Kovtun,<sup>‡</sup> Mykola P. Shandura,<sup>‡</sup> Alexey D. Kachkovski,<sup>‡</sup> David J. Hagan,<sup>‡</sup> Eric W. Van Stryland,<sup>‡</sup> and Anna Painelli<sup>\*,†</sup>

<sup>†</sup>Dipartimento di Chimica GIAF and INSTM UdR-Parma, Università di Parma, Parco Area delle Scienze 17/a, 43124 Parma, Italy,

<sup>§</sup>Institute of Physics, National Academy of Sciences, Kiev 03028, Ukraine, <sup>‡</sup>CREOL, The College of Optics and Photonics, University of Central Florida, Orlando, Florida 32826, and <sup>‡</sup>Institute of Organic Chemistry, National Academy of Sciences, Kiev 03094, Ukraine

**ABSTRACT** Optical spectra of two families of symmetrical polymethine dyes, bearing a positive and a negative charge, are analyzed based on an essential-state model recently developed for quadrupolar dyes. The model accounts for molecular vibrations and polar solvation and reproduces the anomalous evolution with solvent polarity of experimental absorption band shapes. Fluorescence and excited-state absorption spectra are well-described within the same model, which also quantitatively reproduces the recent observation of an intense two-photon absorption toward the (two-photon forbidden) lowest excited state. An extensive analysis of optical spectra demonstrates that the essential-state model developed for quadrupolar dyes also applies to polymethine dyes and that long polymethine dyes offer the first experimental example of class III quadrupolar chromophores.

**SECTION** Statistical Mechanics, Thermodynamics, Medium Effects



Polymethine dyes (PDs), with their intense absorption tunable from the visible to the near-infrared, are the subjects of intense interest for several rewarding applications.<sup>1,2</sup> Theoretical studies of PDs date back to almost a century,<sup>3</sup> and while different approaches were adopted, it is now clear that the physics of PDs is governed by a subtle interplay between delocalized electrons and molecular vibrations. In this respect, PDs share some basic physics with  $\pi$ -conjugated polymers; PDs have been already described as  $\pi$ -conjugated compounds with solitonic-like behavior, bearing either positive or negative charges, depending on terminal groups.<sup>4</sup> Optical spectra of PDs show an intriguing evolution with the length of the conjugated backbone and/or with the solvent polarity, suggesting that the ground state of long PDs is a broken-symmetry state.<sup>4–6</sup> A quantitative description of optical spectra of PDs is however still missing and requires a detailed modeling of the subtle interplay between delocalized electrons, molecular vibrations, and polar solvation. Recently, models for polar<sup>7</sup> and multipolar<sup>8,9</sup> chromophores in solution were proposed that, accounting for just a few electronic states, successfully describe molecular vibrations and polar solvation. Quite interestingly, the model for quadrupolar chromophores (a family of linear  $\pi$ -conjugated molecules with general structure D- $\pi$ -A- $\pi$ -D or A- $\pi$ -D- $\pi$ -A, where D and A represent electron-donor and acceptor groups, connected by  $\pi$ -conjugated bridges) supports symmetry breaking. Specifically, according to ref 8, quadrupolar dyes can be classified in three different families with distinctively different spectroscopic behavior. Class I dyes,

represented, for example, by fluorene-based dyes, undergo symmetry breaking in the first excited state. Absorption spectra of class I dyes, involving vertical (unrelaxed) nonpolar states, are therefore nonsolvatochromic. Fluorescence, however, occurs from the relaxed excited state, corresponding to a broken-symmetry polar state. Class II dyes then show a strong fluorescence solvatochromism.<sup>8</sup> Class II chromophores, squaraine-based dyes being typical examples, are not prone to symmetry breaking; their ground and excited states maintain a symmetric charge distribution, and their optical spectra are only marginally affected by solvent polarity.<sup>8</sup> The third class of chromophores undergoes symmetry breaking in the ground state; large polarity effects are expected on absorption spectra of class III dyes. However, so far, examples of class III dyes have not been recognized. In this work, a quantitative analysis of optical spectra of PDs demonstrates that the essential-state model developed for quadrupolar dyes also applies to PDs and that long PDs are representatives of class III chromophores.

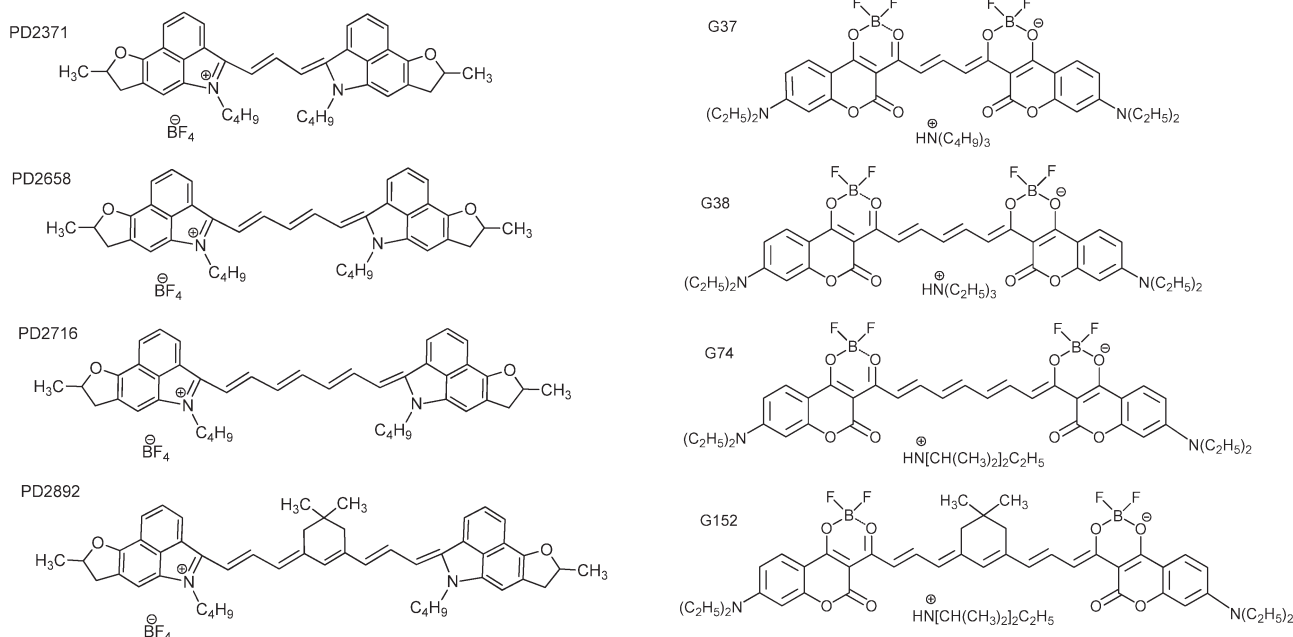
Optical spectra of PDs are complex due to the presence of many low-energy excited states.<sup>10,11</sup> However, similar to conjugated polymers, linear and nonlinear optical spectra of PDs are mainly dominated by two excited states.<sup>12</sup> The first essential excited state, corresponding to the  $1B_u$  state of

Received Date: April 2, 2010

Accepted Date: May 19, 2010

Published on Web Date: May 25, 2010

Chart 1. Molecular Structures of Anionic (PD Series, Left) and Cationic (G Series, Right) Dyes



conjugated polymers,<sup>12</sup> coincides with the lowest one-photon allowed state. It is characterized by a large transition dipole moment from the ground state and dominates the one-photon absorption (1PA) spectrum. The second essential excited state is a dark state, inactive in 1PA but active in two-photon absorption (2PA). It is characterized by a large transition dipole moment from the  $1B_u$  state and therefore dominates the 2PA spectrum. Similar to the so-called  $mA_g$  state of conjugated polymers,<sup>12</sup> it is higher in energy than the 1PA state and does not coincide with the lowest 2PA state. This picture is supported by excited-state absorption (ESA) spectra; ESA spectra of PDs<sup>10,11</sup> are largely dominated by a single band. The minimal model for PDs then accounts for just three essential electronic states, analogous to the essential states selected to describe quadrupolar chromophores.<sup>8</sup> While seemingly unrelated, PDs and quadrupolar chromophores can be described by the same model, based on just three electronic states with similar symmetry properties, as discussed below.

The model is general and applies to symmetric PDs, irrespective of the terminal groups and/or the total molecular charge. For the sake of clarity, here, we explicitly address the case of charged PDs, and more specifically, we make reference to two families of dyes with different conjugation lengths, the PD series, bearing a positive charge,<sup>10,13</sup> and the G series, bearing a negative charge,<sup>14</sup> as depicted in Chart 1. The three basis (diabatic) states of the model are defined by the two degenerate states where the positive (PD series) or negative (G series) charge is located on one of the terminal groups (corresponding to  $Z_1$  and  $Z_2$  states of ref 8) and by the state where the charge is located in the middle of the chain (corresponding to state N of ref 8). An energy gap  $2\eta$  separates the degenerate  $Z_i$  states from N, while a matrix element  $\tau$  mixes  $Z_1$  and  $Z_2$  with N. The two degenerate states

are conveniently combined into a symmetrical and an antisymmetrical state,  $Z_+$  and  $Z_-$ , respectively.<sup>8</sup> The ground state, G, is a mixture of the two symmetrical states, N and  $Z_+$ . The first excited state, C, coincides with  $Z_-$ . The  $G \rightarrow C$  transition is 1PA-allowed, with a transition dipole moment of  $\mu_{GC} = \mu_0 \rho^{1/2}$ , where  $\mu_0$  is the effective dipole moment associated with the displacement of an electronic charge from the middle of the molecule toward one of the two terminal groups and  $\rho$  is the weight of  $Z_+$  in the ground state. Finally E, the highest-energy state, is again a linear combination of the two symmetrical basis states (N and  $Z_+$ ). It is 1PA-forbidden and 2PA-allowed. The transition dipole moment between C and E,  $\mu_{CE} = -\mu_0(1 - \rho)^{1/2}$ , has a similar magnitude as  $\mu_{GC}$ , at least as long as  $\rho$  significantly deviates from the limits  $\rho \rightarrow 0$  (where G coincides with N) and  $\rho \rightarrow 1$  (where G coincides with  $Z_+$ ).

The molecule readjusts its geometry according to the charge distribution along the molecular backbone. The minimal vibronic model accounts for two equivalent vibrational coordinates,  $Q_1$  and  $Q_2$ , which describe the relaxation of the molecular geometry when the charge moves from the center of the molecule toward each one of the two terminal groups. The relevant relaxation energy is  $\epsilon_v$ , while  $\omega_v$  is the vibrational frequency.<sup>7,8</sup> The two coordinates are combined to account for symmetry,  $Q_{\pm} = (Q_1 \pm Q_2)/2^{1/2}$ . The antisymmetrical coordinate,  $Q_-$ , mixes states of different symmetry and can drive symmetry breaking.<sup>8,15,16</sup>

The solvent is described as an elastic continuum medium, perturbed by the interaction with the solute.<sup>8</sup> The solute charge distribution is expanded in terms of monopolar and dipolar charges located at the molecular center. The monopole charge is invariant in all basis states and becomes irrelevant in the subsequent discussion. Therefore, only dipolar

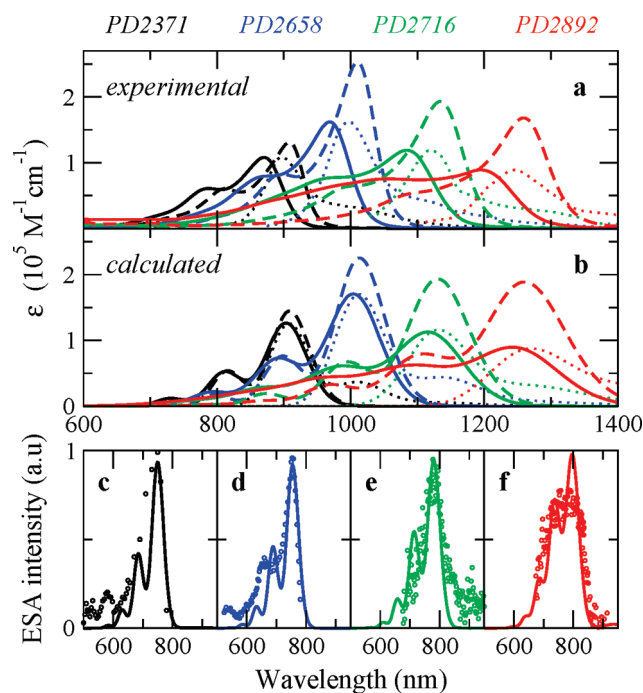


**Figure 1.** Spectra for PD2371 (black), PD2658 (blue), PD2716 (green), and PD2892 (red). (a) Experimental 1PA spectra in acetonitrile (full lines) and *ortho*-dichlorobenzene (dashed lines) and fluorescence spectra in acetonitrile (dotted lines, arbitrary units). (b) Calculated 1PA and fluorescence spectra (same codes as panel a). (c–f) Experimental (symbols) and calculated (full lines) ESA spectra in acetonitrile. Experimental data are from ref 13.

contributions must be accounted for, as in the standard model.<sup>8</sup> The solvation Hamiltonian can be expressed as

$$H_{\text{solv}} = -\hat{\mu}F_R + \frac{\mu_0^2}{4\epsilon_{\text{or}}} F_R^2$$

where the first term couples the reaction field  $F_R$  to the molecular dipole moment operator,  $\hat{\mu}$ . The last term in  $H_{\text{solv}}$  represents the elastic potential energy, where  $\epsilon_{\text{or}}$  is the solvent relaxation energy.  $F_R$  mixes states with different symmetry and cooperates with  $Q_-$  in driving symmetry breaking.  $F_R$  is related to the orientation of polar solvent molecules surrounding the solute; the relevant dynamics is slow, and  $F_R$  can be treated as a classical parameter associated with a thermal distribution.<sup>7,8</sup> Specifically, to account for thermal disorder, the model is defined on a grid of  $F_R$  values. The molecular Hamiltonian describing the three electronic basis states,  $N$ ,  $Z_+$ , and  $Z_-$ , coupled to the vibrational coordinates  $Q_+$  and  $Q_-$ , is then numerically diagonalized (in the nonadiabatic basis) on each point of the grid to obtain  $F_R$ -dependent energies and spectra.<sup>8</sup> Solution spectra are finally calculated summing up the  $F_R$ -dependent spectra, assuming a Boltzmann distribution on relevant energies. The solution is described as a distribution of solute molecules, each one experiencing a slightly different reaction field due to thermal fluctuations of the surrounding solvent. Thermal fluctuations are then responsible for inhomogeneous spectral broadening.

Figures 1 and 2 summarize the results obtained for the two families of compounds in Chart 1. The adopted model is

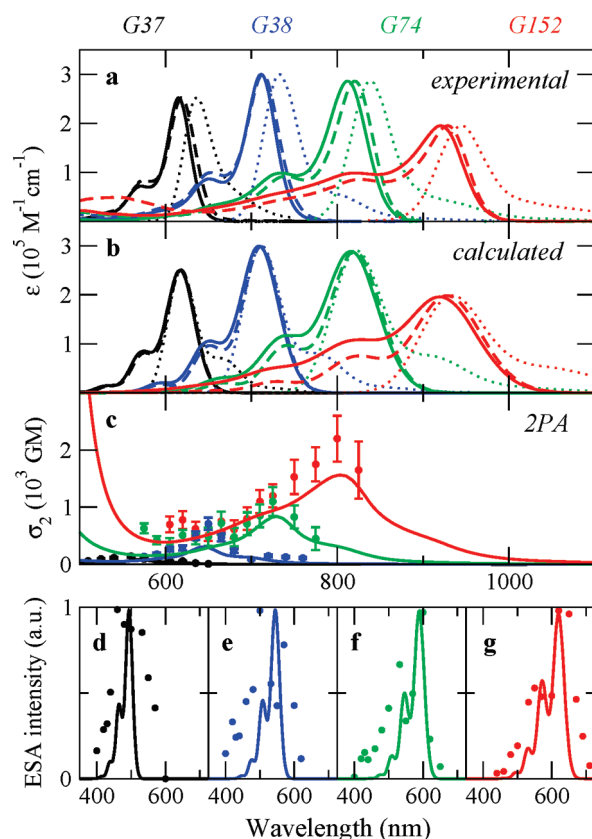


**Figure 2.** Spectra for G37 (black), G38 (blue), G74 (green), and G152 (red). (a) Experimental 1PA spectra in acetonitrile (full lines) and methylene chloride (dashed lines) and fluorescence spectra in acetonitrile (dotted lines, arbitrary units). (b) Calculated 1PA and fluorescence spectra (same codes as panel a). (c) Experimental (symbols and error bars) and calculated (full lines) 2PA spectra (the *x*-axis shows the transition wavelength, that is, half of the wavelength of the absorbed photons;  $1\text{GM} = 10^{-50} \text{cm}^4 \text{s photon}^{-1}$ ). (d–g) Experimental (symbols) and calculated (full lines) ESA spectra in acetonitrile. Experimental data are from ref 14.

semiempirical, and the parameters collected in Table 1 are adjusted to reproduce experimental spectra. For each compound, the positions of 1PA and ESA bands fix the magnitude of  $\tau$  and  $\rho$  (cf. eq 5 of ref 8). The vibrational parameters  $\omega_v$  and  $\epsilon_v$  are tuned to reproduce the vibronic band shapes. The  $\eta$  parameter is adjusted to obtain the required  $\rho$  and hence to locate the absorption band (cf. eqs 4 and 5 of ref 8). The solvent relaxation energy is adjusted for each family of compounds to reproduce the absorption solvatochromism. Finally, a line width  $\Gamma$  is assigned to each vibronic band, while  $\mu_0$  is determined from the molar extinction coefficient.<sup>8</sup> The quality of the model is best appreciated in comparison with the well-known Marcus–Hush (MH) model.<sup>17</sup> In the MH model, the absorption band of a dye is described in terms of five parameters (the optical frequency, the transition dipole moment, the vibrational frequency, the relaxation energy, and the intrinsic line width) that can be directly extracted from experimental data. The MH model parameters depend on the solvent, and a set of five parameters has to be independently optimized to reproduce the absorption band in each solvent. As a result, in the MH model, the calculation of

**Table 1.** Model Parameters for PD and G Series of Molecules

dyes	solvent-independent parameters						solvent parameter $\epsilon_{or}$ [eV] <i>o</i> -DCB/DCM <sup>i</sup> -ACN <sup>j</sup>
	$\eta$ [eV]	$\tau$ [eV]	$\omega_v$ [eV]	$\epsilon_v$ [eV]	$\Gamma$ [eV]	$\mu_0$ [D]	
PD2371 <sup>a</sup>	0.050	1.05	0.150	0.5600	0.05	17.0	0.1–0.23
PD2658 <sup>b</sup>	-0.020	0.99	0.150	0.5700	0.05	22.0	0.1–0.23
PD2716 <sup>c</sup>	-0.060	0.92	0.140	0.5800	0.05	22.0	0.1–0.23
PD2892 <sup>d</sup>	-0.100	0.86	0.120	0.6000	0.05	25.0	0.1–0.23
G37 <sup>e</sup>	-0.080	1.58	0.155	0.4880	0.06	19.6	0.2–0.3
G38 <sup>f</sup>	-0.085	1.40	0.160	0.5256	0.06	23.5	0.2–0.3
G74 <sup>g</sup>	-0.110	1.25	0.160	0.5625	0.06	26.4	0.2–0.3
G152 <sup>h</sup>	-0.130	1.14	0.160	0.6400	0.06	28.3	0.2–0.3

<sup>a</sup> 5-Butyl-4-[3-(5-butyl-8-methyl-7,8-dihydrobenzo[*cd*]furo[2,3-*f*]indol-4(5H)-ylidene)prop-1-enyl]-8-methyl-7,8-dihydrobenzo[*cd*]furo[2,3-*f*]indol-5-ium tetrafluoroborate. <sup>b</sup> 5-Butyl-4-[5-(5-butyl-8-methyl-7,8-dihydrobenzo[*cd*]furo[2,3-*f*]indol-4(5H)-ylidene)penta-1,3-dienyl]-8-methyl-7,8-dihydrobenzo[*cd*]furo[2,3-*f*]indol-5-ium tetrafluoroborate. <sup>c</sup> 5-Butyl-4-[7-(5-butyl-8-methyl-7,8-dihydrobenzo[*cd*]furo[2,3-*f*]indol-4(5H)-ylidene)hepta-1,3,5-trienyl]-8-methyl-7,8-dihydrobenzo[*cd*]furo[2,3-*f*]indol-5-ium tetrafluoroborate. <sup>d</sup> 5-Butyl-4-(3-{3-[3-(5-butyl-8-methyl-7,8-dihydrobenzo[*cd*]furo[2,3-*f*]indol-4(5H)-ylidene)prop-1-enyl]-5,5-dimethylcyclohex-2-en-1-ylidene}prop-1-enyl)-8-methyl-7,8-dihydrobenzo[*cd*]furo[2,3-*f*]indol-5-ium tetrafluoroborate. <sup>e</sup> Tributylammonium 2,2-difluoro-4-[3-(8-(diethylamino)-2,2-difluoro-5-oxo-(5H)-chromeno[4,3-*d*]-1,3,2-(2H)-dioxaborin-4-ylidene)-1-propenyl]-5-oxo-(5H)-8-(diethylamino)-chromeno[4,3-*d*]-1,3,2-(2H)-dioxaborinate. <sup>f</sup> Triethylammonium 2,2-difluoro-4-[5-(8-(diethylamino)-2,2-difluoro-5-oxo-(5H)-chromeno[4,3-*d*]-1,3,2-(2H)-dioxaborin-4-ylidene)-1,3-pentadienyl]-8-(diethylamino)-5-oxo-(5H)-chromeno[4,3-*d*]-1,3,2-(2H)-dioxaborinate. <sup>g</sup> Diisopropylethylammonium 2,2-difluoro-4-[7-(2,2-difluoro-5-oxo-(5H)-8-(diethylamino)-chromeno[4,3-*d*]-1,3,2-(2H)-dioxaborin-4-ylidene)-1,3,5-heptatrienyl]-5-oxo-(5H)-8-(diethylamino)-chromeno[4,3-*d*]-1,3,2-(2H)-dioxaborinate. <sup>h</sup> Diisopropylethylammonium 2,2-difluoro-4-[4,6-(2,2-dimethyl)-trimethylen-9-(2,2-difluoro-5-oxo-(5H)-8-(diethylamino)-chromeno[4,3-*d*]-1,3,2-(2H)-dioxaborin-4-ylidene)-1,3,5,7-nonanotetraenyl]-5-oxo-(5H)-8-(diethylamino)-chromeno[4,3-*d*]-1,3,2-(2H)-dioxaborinate. <sup>i</sup> *ortho*-Dichlorobenzene (*o*-DCB, for PD series)/dichloromethane (DCM, for G series). <sup>j</sup> Acetonitrile (ACN, for both series).

just the absorption bands collected in  $n$  solvents requires  $5 \times n$  adjustable parameters for each dye. In our model, instead, six solvent-independent molecular parameters are needed for each dye to calculate optical spectra in solution, plus a single solvent-dependent parameter,  $\epsilon_{or}$ , for a grand-total of  $6 + n$  parameters (cf. Table 1). Of course, the higher the number of solvents, the bigger the gain of our model with respect to the MH model. The power of the essential-state model is recognized not only in the reduction of the number of model parameters but even more in the possibility to address many (potentially all) low-energy spectral properties in a unique and coherent picture. Specifically, the model parameters in Table 1 allow for the calculation of absorption, fluorescence, and ESA and 2PA spectra for the two families of compounds (cf. Figures 1 and 2; 2PA spectra are not shown for the PD series because of the lack of experimental data). The MH parameters refer to the adiabatic ground and excited states of the solvated molecule and are directly related to experimental observables (e.g., the relaxation energy is half of the observed Stokes shift). In contrast, the solvent-independent parameters of essential-state models refer to the diabatic basis states and, being not directly related to experimental observables, are fixed by a global fit of spectral properties.

The proposed model naturally explains the anomalous evolution with the solvent polarity of absorption spectra of both families of compounds in Chart 1. The broad shoulder that appears in polar solvents on the blue side of the main absorption band is related to the presence in solution of molecules in a broken-symmetry state. Figure 3 shows the distribution of the reaction field calculated for the two series of compounds. For each dye, as the solvent polarity increases, the distribution of the reaction field relevant to the ground state broadens considerably, resulting in an increasing population of molecules in

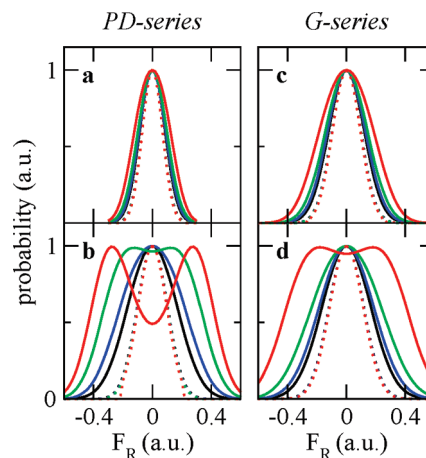


**Figure 3.** Left panels: probability distributions for the reaction field calculated for the compounds of the PD series (color code as that in Figure 1) for  $\epsilon_{or} = 0.1$  (a) and  $\epsilon_{or} = 0.2$  (b). Right panels: probability distributions for the reaction field calculated for the compounds of the G series (color code as that in Figure 2) for  $\epsilon_{or} = 0.2$  (c) and  $\epsilon_{or} = 0.23$  (d). In all panels, continuous lines refer to the ground-state distribution, while dotted lines refer to distributions relevant to the first excited state.

a polar, broken-symmetry state. This phenomenon is particularly important for long-chain molecules, where the appearance of a bimodal distribution signals the occurrence of true symmetry breaking with polar states lower in energy than symmetry-conserving nonpolar states.

The model, optimized to reproduce 1PA and ESA spectra, applies to the calculation of other spectral properties as well. In particular, the same model that explains the broad and solvent-dependent absorption spectra of both PD and G series of compounds elucidates the narrow and almost

solvent-independent fluorescence and ESA spectra observed for all compounds. In fact, both fluorescence and ESA processes start from the first excited state, which for class III dyes is not prone to symmetry breaking. As shown in Figure 3 (dotted lines), the relevant  $F_{or}$  distribution is narrow, quite irrespective of the chain length.

Even more impressive are the results obtained for 2PA. Experimental data available for the G series<sup>13</sup> are shown in Figure 2. We concentrate attention on the lowest-energy 2PA band occurring in the blue wing of the 1PA. The 2PA cross section ( $\sigma_2$ ) associated with this nominally forbidden band in the 1PA region is very high, exceeding 2000 GM for G152. Our model accurately reproduces the position, intensity, and location of this band. The agreement is particularly good with reference to the evolution of the 2PA spectra with the chain length. Two main mechanisms are responsible for the sizable 2PA intensity of the nominally 2PA-forbidden  $G \rightarrow C$  transition. The first mechanism is related to vibronic coupling driven by the antisymmetric  $Q_-$  vibration.<sup>18</sup> The relevant 2PA intensity increases with the conjugation length and hence with the effectiveness of vibrational coupling.<sup>19</sup> The second mechanism is related to symmetry breaking in polar solvents; the wide and sometimes bimodal distributions of reaction fields calculated for the ground state imply a sizable population of molecules in a broken-symmetry state. The  $G \rightarrow C$  transition becomes two-photon allowed for these molecules, and its intensity increases with the chain length because long PDs are more prone to symmetry breaking.

In summary, the proposed model quantitatively reproduces the anomalous evolution with the solvent polarity of ground-state absorption spectra of symmetrical cationic and anionic series of polymethine dyes, as well as their fluorescence and ESA spectra. The model also quantitatively reproduces the lowest-energy 2PA band measured for the series of anionic dyes. Polymethine dyes with long chains undergo symmetry breaking in the ground state and offer the first experimental example of class III quadrupolar chromophores.

## AUTHOR INFORMATION

### Corresponding Author:

\*To whom correspondence should be addressed. E-mail: anna.painelli@unipr.it.

**ACKNOWLEDGMENT** Work in Parma is supported by Parma University. U.C.F. gratefully acknowledges support from the U.S. Army Research Laboratory and the U.S. Army Research Office: 50372-CH-MUR.

## REFERENCES

- Mishra, A.; Behera, R. K.; Behera, P. K.; Mishra, B. K.; Behera, G. B. Cyanines During the 1990s: A Review. *Chem. Rev.* **2000**, *100*, 1973–2012.
- Fabian, J.; Nakazumi, H.; Matsuoka, M. Near-Infrared Absorbing Dyes. *Chem. Rev.* **1992**, *92*, 1197–1226.
- See, for example, Brooker, L. G. S. Spectra of Dye Molecules: Absorption and Resonance in Dyes. *Rev. Mod. Phys.* **1942**, *14*, 275–293 and references therein.
- Tolbert, L. M.; Zhao, X. Beyond the Cyanine Limit: Peierls Distortion and Symmetry Collapse in a Polymethine Dye. *J. Am. Chem. Soc.* **1997**, *119*, 3253–3258.
- Lepkowicz, R. S.; Przhonska, O. V.; Hales, J. M.; Fu, J.; Hagan, D. J.; Van Stryland, E. W.; Bondar, M. V.; Slominsky, Y. L.; Kachkovski, A. D. Nature of the Electronic Transitions in Thiocarbocyanines with a Long Polymethine Chain. *Chem. Phys.* **2004**, *305*, 259–270.
- Fabian, J. Symmetry-Lowering Distortion of Near-Infrared Polymethine Dyes — A Study by First Principles Methods. *THEOCHEM* **2006**, *766*, 49–60.
- Boldrini, B.; Cavalli, E.; Painelli, A.; Terenziani, F. Polar Dyes in Solution: A Joint Experimental and Theoretical Study of Absorption and Emission Shapes. *J. Phys. Chem A* **2002**, *106*, 6286–6294.
- Terenziani, F.; Painelli, A.; Katan, C.; Charlot, M.; Blanchard-Desce, M. Charge Instability in Quadrupolar Chromophores: Symmetry Breaking and Solvatochromism. *J. Am. Chem. Soc.* **2006**, *128*, 15742–15755.
- Terenziani, F.; Sissa, C.; Painelli, A. Symmetry Breaking in Octupolar Chromophores: Solvatochromism and Electroabsorption. *J. Phys. Chem. B* **2008**, *112*, 5079–5087.
- Padilha, L. A.; Webster, S.; Hu, H.; Przhonska, O. V.; Hagan, D. J.; Van Stryland, E. W.; Bondar, M. V.; Davydenko, I. G.; Slominsky, Y. L.; Kachkovski, A. D. Excited State Absorption and Decay Kinetics of Near IR Polymethine Dyes. *Chem. Phys.* **2008**, *352*, 97–105.
- Webster, S.; Fu, J.; Padilha, L. A.; Przhonska, O. V.; Hagan, D. J.; Van Stryland, E. W.; Bondar, M. V.; Slominsky, Y. L.; Kachkovski, A. D. Comparison of Nonlinear Absorption in Three Similar Dyes: Polymethine, Squaraine and Tetraone. *Chem. Phys.* **2008**, *348*, 143–151.
- Dixit, S. N.; Guo, D.; Mazumdar, S. Essential State mechanism of Optical Non-Linearity in  $\pi$ -Conjugated Polymers. *Phys. Rev. B* **1991**, *43*, 6781.
- Webster, S.; Padilha, L. A.; Hu, H.; Przhonska, O. V.; Hagan, D. J.; Van Stryland, E. W.; Bondar, M. V.; Davydenko, I. G.; Slominsky, Y. L.; Kachkovski, A. D. Structure and Linear Spectroscopic Properties of Near IR Polymethine Dyes. *J. Lumin.* **2008**, *128*, 1927–1936.
- Padilha, L. A.; Webster, S.; Przhonska, O. V.; Hu, H.; Peceli, D.; Ensley, T. R.; Bondar, M. V.; Gerasov, A. O.; Kovtun, Y. P.; Shandura, M. P.; et al. Efficient Two-Photon Absorbing Acceptor- $\pi$ -Acceptor Polymethine Dyes. *J. Phys. Chem. A* ASAP article, DOI: 10.1021/jp100963e.
- Foulton, R. M.; Gouterman, M. Vibronic coupling. I. Mathematical Treatment for Two Electronic States. *J. Chem. Phys.* **1961**, *35*, 1059–1071.
- Iordanov, T. D.; Davis, J. L.; Masunov, A. E.; Levenson, A.; Przhonska, O. V.; Kachkovski, A. D. Symmetry Breaking in Cationic Polymethine Dyes: Ground State Potential Energy Surfaces and Solvent Effects on Electronic Spectra of Streptocyanines. *Int. J. Quantum Chem.* **2009**, *109*, 3592–3601.
- Bixon, M.; Jortner, J. Electron Transfer. From Isolated Molecules to Biomolecules. *J. Adv. Chem. Phys.* **1999**, *106*, 35–202.
- Painelli, A.; Del Freato, L.; Terenziani, F. Vibronic Contributions to Resonant NLO Responses: Two-Photon Absorption in Push-Pull Chromophores. *Chem. Phys. Lett.* **2001**, *346*, 470–478.
- Girlando, A.; Painelli, A.; Soos, Z. G. Electron-Phonon Coupling in Conjugated Polymers: Reference Force Field and Transferable Coupling Constants for Polyacetylene. *J. Chem. Phys.* **1993**, *98*, 7459–7465.